

Deuterium isotope effect on femtosecond solvation dynamics in methyl β - cyclodextrins

Dibyendu Kumar Sasmal, Shantanu Dey, Dibyendu Kumar Das, and Kankan Bhattacharyya

Citation: *The Journal of Chemical Physics* **131**, 044509 (2009); doi: 10.1063/1.3176020

View online: <http://dx.doi.org/10.1063/1.3176020>

View Table of Contents: <http://scitation.aip.org/content/aip/journal/jcp/131/4?ver=pdfcov>

Published by the [AIP Publishing](#)

Articles you may be interested in

[Photoisomerization among ring-open merocyanines. I. Reaction dynamics and wave-packet oscillations induced by tunable femtosecond pulses](#)

J. Chem. Phys. **140**, 224310 (2014); 10.1063/1.4881258

[On the origin of ultrafast nonradiative transitions in nitro-polycyclic aromatic hydrocarbons: Excited-state dynamics in 1-nitronaphthalene](#)

J. Chem. Phys. **131**, 224518 (2009); 10.1063/1.3272536

[Ultrafast excited-state dynamics of tetraphenylethylene studied by semiclassical simulation](#)

J. Chem. Phys. **127**, 094307 (2007); 10.1063/1.2768347

[Dissociation dynamics of thiolactic acid at 193 nm: Detection of the nascent OH product by laser-induced fluorescence](#)

J. Chem. Phys. **120**, 6964 (2004); 10.1063/1.1667878

[Deuterium isotope effect on the solvation dynamics of a dye molecule in methanol and acetonitrile](#)

J. Chem. Phys. **110**, 10969 (1999); 10.1063/1.479034



Deuterium isotope effect on femtosecond solvation dynamics in methyl β -cyclodextrins

Dibyendu Kumar Sasmal, Shantanu Dey, Dibyendu Kumar Das, and Kankan Bhattacharyya^{a)}

Department of Physical Chemistry, Indian Association for the Cultivation of Science, Jadavpur, Kolkata 700 032, India

(Received 8 May 2009; accepted 20 June 2009; published online 24 July 2009)

Deuterium isotope effect on the solvation dynamics and fluorescence anisotropy decay of coumarin 153 (C153) bound to dimethyl β -cyclodextrin (DMB) and trimethyl β -cyclodextrin (TMB) is studied using femtosecond upconversion. In D_2O , there is a marked increase in the steady state emission quantum yield and fluorescence lifetime of C153 bound to DMB and TMB. This suggests strong coupling between C153 and D_2O inside the cyclodextrin cavity. In D_2O , average solvation time of C153 in DMB is about 1.7 times slower compared to that in water. For TMB in D_2O , solvation is 1.5 times slower. The deuterium isotope effect on solvation dynamics at long time arises mainly from the longer excited state lifetime. The longest components of solvation dynamics are ascribed to self-diffusion of C153 out of the cyclodextrin cavity. The nearly 1.5 times slower anisotropy decay of C153 bound to DMB and TMB in D_2O (compared to H_2O) is attributed to higher viscosity of D_2O . © 2009 American Institute of Physics. [DOI: 10.1063/1.3176020]

I. INTRODUCTION

In recent years, there are many reports on the dramatic slowing down of solvation dynamics of confined water molecules in a nanocavity.^{1–40} The ultraslow component of solvation dynamics in a nanocavity is slower by two to three orders of magnitude compared to the subpicosecond dynamics in bulk water. In general, the ultraslow component of confined water environment has been attributed to immobilization of water and interconversion of bound and free water.^{30–40} Golosov and Karplus⁴¹ suggested that the slow solvation dynamics in an aqueous solution of a protein arises from the motion of the polar residues of a protein. Rodriguez *et al.*⁴² carried out a detailed computer simulation on solvation dynamics in methylated β -cyclodextrin. They argued that the slow dynamics arises from the change in conformation of the hydroxyl groups of the cyclodextrin cavity.⁴² In this work, we report on deuterium isotope effect on solvation dynamics in methyl cyclodextrin.

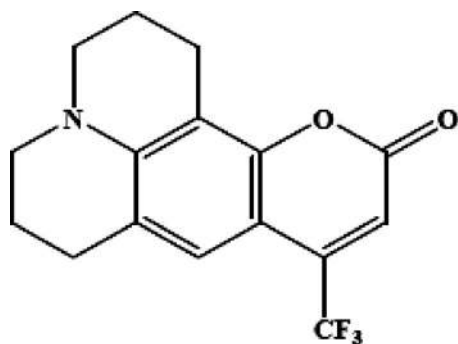
The structure of D_2O has been extensively investigated by experiments⁴³ and theory.⁴⁴ Most recently, using x-ray diffraction, neutron diffraction, and computer simulation, Soper and Benmore⁴³ showed that the individual hydrogen (deuterium) bonds in D_2O is $\sim 4\%$ longer (weaker) than those in H_2O . However, the number of hydrogen bonds a D_2O molecule makes (3.76) is larger than those (3.62) in H_2O .⁴³ This makes D_2O more structured than H_2O . As a result of this, hydrophobic effect is stronger in D_2O and the binding constant of an organic guest to cyclodextrin is larger in D_2O compared to H_2O .^{45,46}

Previously many groups have studied deuterium isotope effect on solvation dynamics in bulk water,^{47,48} aqueous suspension of ZrO_2 nanoparticle,⁴⁷ methanol,^{49,50} micelle,⁵¹ re-

verse micelle,⁵² and anisotropy decay in water.⁵³ They showed that the solvation dynamics is $\sim 25\%$ slower in D_2O compared to H_2O . The dielectric relaxation of D_2O is $\sim 25\%$ slower compared to H_2O .⁵⁴ Nandi *et al.*⁵⁵ used a molecular hydrodynamic theory while Schwartz and Rossky⁵⁶ carried out a quantum nonadiabatic molecular dynamic simulations to explain the deuterium isotope effect on solvation dynamics. According to these theoretical studies, the ultrafast subpicosecond response of bulk water^{55–59} originates from strong solvent-solute coupling and the extended hydrogen bond network in bulk water. It is proposed that deuterium substitution slows down solvation dynamics by modifying the intermolecular libration frequencies.^{55,56} Another consequence of deuteration is slowing down of the nonradiative transitions and consequent increase in the excited state lifetime.⁵⁶ This is primarily due to the slower solvation in D_2O which keeps the energy gap between the excited and ground state high for a longer time.⁵⁶

There are three hydroxyl groups in β -cyclodextrin, an exposed primary (O6) group near the narrower rim and two secondary, sterically hindered ones (O2 and O3), located near the wider rim. In dimethyl β -cyclodextrin (DMB), the O6 and O2 are methylated while in trimethyl β -cyclodextrin (TMB), all the three hydroxyl groups are converted into methoxy group. Methylated cyclodextrins are far more soluble in water compared to unsubstituted cyclodextrins.^{60–62} They are widely used in drug delivery⁶⁰ and to prevent misfolding of a protein.⁶¹ The solubility of a methylated cyclodextrin exhibits negative temperature coefficient, i.e., decreases with increase in temperature.⁶² If DMB is crystallized from an aqueous solution at a low temperature ($18^\circ C$), a hydrated crystal with 15 water molecules of crystallization (DMB.15 H_2O) is obtained.⁶² However, if a concentrated aqueous solution of DMB is heated (to

^{a)}Electronic mail: pckb@iacs.res.in. FAX: (91)-33-2473-2805.

**C153**

SCHEME 1. Schematic representation of C153.

50°–70 °C) completely anhydrous DMB crystal is obtained.^{63–65} According to computer simulation^{42,62} and X-ray crystallography^{63–65} water molecules do not penetrate the cavity of the methylated cyclodextrins. Instead at low temperature, water molecules form a clathratelike structure around DMB and TMB.^{62–65}

In this work, we investigate whether a guest molecule (coumarin 153, C153) bound to DMB and TMB are exposed to water molecules at low temperature (20 °C) and whether the solvation dynamics of C153 in DMB and TMB exhibit any deuterium isotope effect. We carried out the experiment at 20 °C where a lot of water molecules remain bound to DMB and TMB.^{62–65}

II. EXPERIMENTAL SECTION

Coumarin 153 (C153, Exciton, Scheme 1), heptakis (2,3,6-tri-O-methyl)-β-cyclodextrin (TMB, Fluka) and dimethyl-β-cyclodextrin (DMB, Aldrich) were used as received. A small amount of C153 was added to double distilled water or D₂O and was sonicated for half an hour. After that the solution was allowed to stand for half an hour. Then the clear upper part of the solution was decanted and the decanted solution was used for our experiments. The steady state absorption and emission spectra were recorded in a Shimadzu UV-2401 spectrophotometer and a Spex FluoroMax-3 spectrofluorimeter, respectively.

Our femtosecond upconversion setup (FOG 100, CDP) is described earlier.²⁹ Briefly, in our femtosecond upconversion setup (FOG 100, CDP) the sample was excited at 405 nm using the second harmonic of a mode-locked Ti-sapphire laser (Tsunami, Spectra Physics), pumped by a 5 W Millennia (Spectra Physics). In order to generate second harmonic we used a nonlinear crystal (1 mm β-Barium Borate BBO, θ=25°, φ=90°). The fluorescence emitted from the sample was upconverted in a nonlinear crystal (0.5 mm BBO, θ=38°, φ=90°) using the fundamental beam as a gate pulse. The upconverted light is dispersed in a monochromator and detected using photon counting electronics. A cross-correlation function obtained using the Raman scattering from ethanol displayed a full width at half maximum (FWHM) of 350 fs. The femtosecond transients were fitted using a Gaussian shape for the exciting pulse.

To determine the picosecond components, the samples were excited at 405 nm using a picosecond diode laser (IBH nanoled) in an IBH Fluorocube apparatus. The emission was collected at a magic angle polarization using a Hamamatsu MCP photomultiplier (5000U-09). The time correlated single photon counting setup consists of an Ortec 9327 CFD and a Tennelec TC 863 TAC. The data is collected with a DAQ-1 MCA card as a multichannel analyzer. The typical FWHM of the system response using a liquid scatterer is about 90 ps. All experiments were done at 20 °C.

In order to fit the femtosecond transient, first we determined the long picosecond component by deconvolution of the picosecond decays (fitted to be a biexponential function using IBH DAS 6 software). Then the long picosecond components were kept fixed to fit the femtosecond data. For the deconvolution and fitting of the femtosecond fluorescence transients we used IGOR PRO 6.04 software. Thus the femtosecond data revealed ultrafast components.

The time resolved emission spectra were constructed using the parameters of best fit to the fluorescence decays and the steady state emission spectrum following the procedure described by Maroncelli and Fleming.⁶⁶ The solvation dynamics is described by the decay of the solvent correlation function $C(t)$, defined as

$$C(t) = \frac{\nu(t) - \nu(\infty)}{\nu(0) - \nu(\infty)}, \quad (1)$$

where $\nu(0)$, $\nu(t)$, and $\nu(\infty)$ are the emission maxima (frequencies) at time 0, t , and ∞ , respectively. Note, a portion of solvation dynamics is missed even in our femtosecond set up of time resolution 350 fs. The amount of solvation missed is calculated using the Fee–Maroncelli procedure.⁶⁷ The emission frequency at time zero, $\nu_{em}^p(0)$ may be calculated using the absorption frequency (ν_{abs}^p) in a polar medium (i.e., C153 in cyclodextrin) as⁶⁷

$$\nu_{em}^p(0) = \nu_{abs}^p - (\nu_{abs}^{np} - \nu_{em}^{np}), \quad (2)$$

where ν_{em}^{np} and ν_{abs}^{np} denote the steady state frequencies of emission and absorption, respectively, of the probe (C153) in a nonpolar solvent (cyclohexane).⁶⁸

In order to study picosecond fluorescence anisotropy decay, the analyzer was rotated at regular intervals to get perpendicular (I_{\perp}) and parallel (I_{\parallel}) components ($\lambda_{em} = 490$ nm). Then the anisotropy function, $r(t)$ was calculated using the formula

$$r(t) = \frac{I_{\parallel}(t) - GI_{\perp}(t)}{I_{\parallel}(t) + 2GI_{\perp}(t)}. \quad (3)$$

The G value of the picosecond set up was determined using a probe whose rotational relaxation is very fast, (e.g., C480 in methanol) and the G value was found to be 1.5.

III. RESULTS

A. Steady state emission spectra

In bulk water, emission intensity of C153 exhibits appreciable deuterium isotope effect. The emission quantum yield (ϕ_f) of C153 in D₂O is 0.21 which is about twofold larger than that⁶⁸ in H₂O ($\phi_f=0.12$) (Fig. 1). The enhancement of

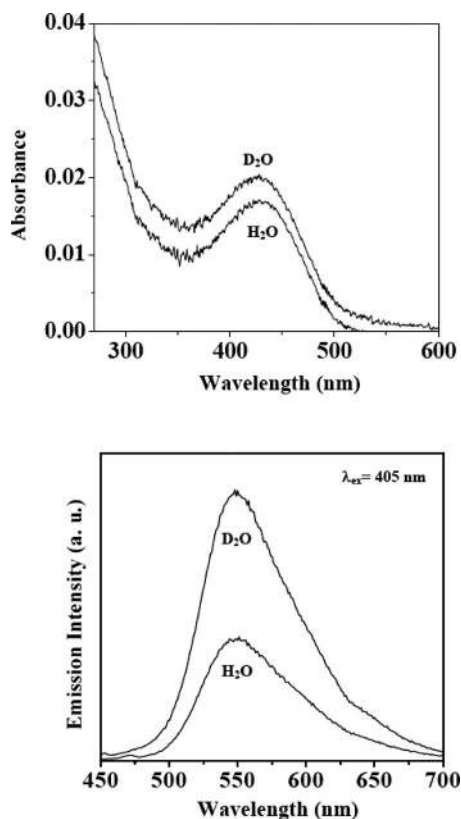


FIG. 1. Steady state absorption and emission spectra of C153 in H₂O and D₂O.

fluorescence may arise from deuterium isotope effect on the nonradiative decay and may be attributed to the lower frequency of the O-D stretch.⁵⁶ The slowing down of nonradiative decay is also manifested in the increase in fluorescence lifetime of C153 (to be discussed later).

Addition of 130 mM cyclodextrin to an aqueous solution of C153 results in a blue shift of the emission maximum from 549 nm in bulk D₂O (or H₂O) to 525 and 522 nm, respectively, in DMB and TMB. The blueshift indicates a lower polarity and more hydrophobic nature of the cyclodextrin cavity compared to bulk D₂O (H₂O). This effect is more

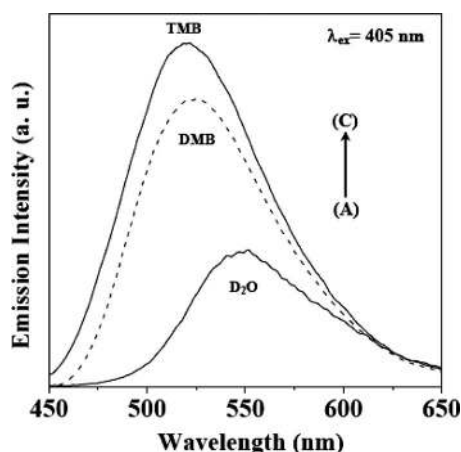


FIG. 2. Steady state emission spectra of C153 ($\lambda_{ex}=405$ nm) in (A) bulk D₂O (—), (B) 130 mM DMB in D₂O (---), and (C) 130 mM TMB in D₂O (· · ·).

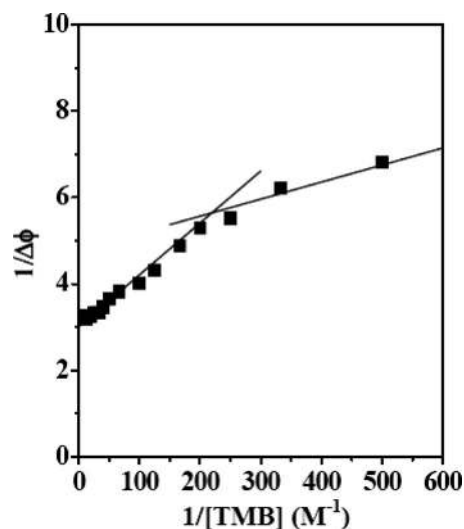


FIG. 3. Plot of $1/\Delta\phi$ vs $1/[TMB]$ for C153 in TMB-D₂O.

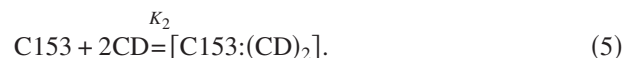
prominent for TMB than that for DMB. This may be attributed to the absence of free hydroxyl groups in the former (TMB). The blue shift is accompanied by an increase in ϕ_f from 0.21 in D₂O to 0.53 in TMB and 0.41 for DMB. Figure 2 shows the emission spectra of C153 in DMB and TMB in D₂O solutions.

The binding equilibrium of C153 to DMB and TMB involves both 1:1 and 1:2 (C153:CD) complexes. The 1:1 host-guest complex corresponds to the following equilibrium:²⁹



The equilibrium constant K_1 , is determined from the double reciprocal plot of change in emission quantum yield ($\Delta\phi$) against CD concentration (Fig. 3). The value of K_1 for 1:1 (C153:CD) complex in D₂O is found to be $250M^{-1}$ and $1330M^{-1}$ (Table I), respectively, for DMB and TMB. Note, the corresponding values of K_1 for DMB and TMB in H₂O are $220M^{-1}$ and $1220M^{-1}$, respectively.²⁹ The slightly higher binding constant in D₂O compared to H₂O is consistent with the previous studies of binding of other guests to methylated cyclodextrins^{45,46} and may be attributed to more solvophobic nature of D₂O.^{43,44}

At higher CD concentrations the slope of the plot (Fig. 3) changes presumably because of the formation of 1:2 complexes $[C153:(CD)_2]$.



If ϕ_0 , ϕ_1 , and ϕ_2 denote emission quantum yields of the solutions containing free C153, 1:1 $[C153:CD]$ complex and 1:2 $[C153:(CD)_2]$ complex, the observed emission quantum yield ϕ is given by

$$\phi = \frac{\phi_0 + \phi_1 K_1 [CD] + \phi_2 K_2 [CD]^2}{1 + K_1 [CD] + K_2 [CD]^2}. \quad (6)$$

The values of ϕ_1 , ϕ_2 , and K_2 were obtained from a nonlinear least square fitting of the plot of ϕ_f against $[CD]$ (Fig. 4). The value of K_2 for the 1:2 $[C153:(CD)_2]$ com-

TABLE I. Binding constants, emission quantum yield, and relative contribution of 1:1 and 1:2 complexes for C153 in 130 mM DMB and TMB in D₂O and H₂O.

	DMB		TMB	
	D ₂ O	H ₂ O	D ₂ O	H ₂ O
K_1^a (M^{-1})	250	220	1330	1220
K_2^a (M^{-2})	3640	3350	40 100	38 500
ϕ_1^a	0.38	0.23	0.42	0.26
ϕ_2^a	0.42	0.33	0.57	0.35
Amt. of free probe ^a	1	1	0.12	0.1
Amt. of probe in 1:1 complex(%) ^a	33	33	20	19.6
Amt. of probe in 1:2 complex(%) ^a	66	66	80	80.3

^a±10%.

plexes is determined to be $3,640M^{-2}$ and $40,100M^{-2}$ for DMB and TMB in D₂O, respectively (Table I). The corresponding values of K_2 in H₂O are $3,350M^{-2}$ and $38,500M^{-2}$, respectively, for DMB and TMB.²⁹ It may be noted that the magnitude of K_2 in D₂O is also higher than that in H₂O for both DMB and TMB.

For a given concentration of CD, the contribution of the probe (C153) in free, 1:1 and 1:2 complexes may be calculated as described earlier.²⁹ For 130 mM DMB in D₂O, 66% of the probe C153 remain bound to DMB as 1:2 complex, 33% in 1:1 complex and only 1% remains free in bulk D₂O. For TMB, 80% of the probe C153 are present in form of 1:2 complex, 20% as 1:1 complex and only ~0.1% remain free in D₂O (Table I).

B. Fluorescence anisotropy decay

In bulk water, C153 exhibits a fast anisotropy decay ($\tau_R \sim 100$ ps).⁶⁹ On binding to 130 mM TMB and DMB the anisotropy decay of C153 becomes substantially slower. The slow anisotropy decay may be attributed to the large size of the cyclodextrin-C153 host-guest complex. Figures 5(a) and 5(b) show the fluorescence anisotropy decays of C153 bound

to DMB and TMB in H₂O and D₂O solution, respectively.

For 130 mM DMB in D₂O, the faster component of anisotropy decay of C153 is ~ 1450 ps (28%) and the slower component is 3600 ps (72%) with an average rotational time ($\langle\tau_R\rangle$) 3000 ps (Table II). It may be recalled²⁹ that in H₂O, C153 bound to DMB displays two components (1150 and 2700 ps) with an average rotational time 2200 ps. This clearly indicates that the anisotropy decay of C153 bound to DMB is 1.4 times slower in D₂O compared to that in water.

For C153 bound to TMB, the faster component of anisotropy decay in D₂O is 1000 ps and the slower component 3150 ps (Table II). In H₂O, the corresponding components are 1000 and 2500 ps.²⁹ The average rotational time of C153 bound to TMB in D₂O ($\langle\tau_R\rangle=2800$ ps) is 1.3 times slower than that in H₂O ($\langle\tau_R\rangle=2200$ ps).

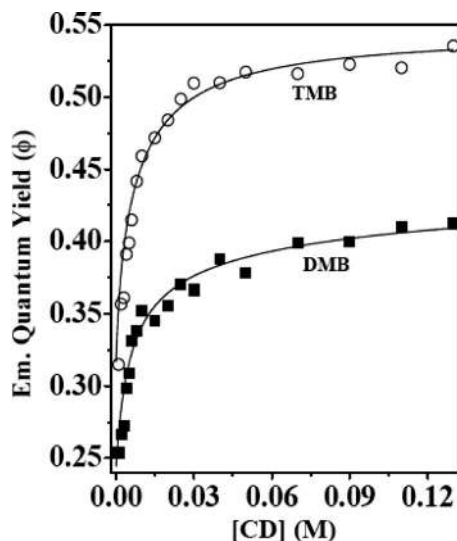


FIG. 4. Plot of emission quantum yield (ϕ) of C153 vs [CD] in D₂O with varying concentration of the CD's (a) DMB (■) and (b) TMB (○). The points represent experimental values and the solid line represents the non linear least square fit corresponding to Eq. (6).

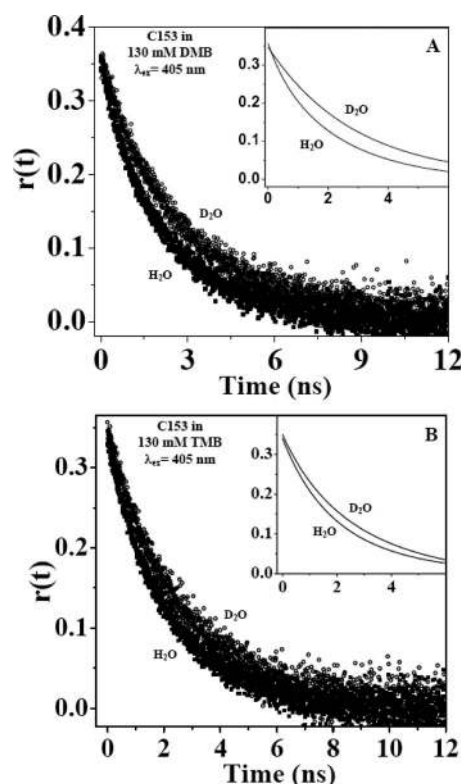


FIG. 5. Fluorescence anisotropy decay of C153 ($\lambda_{ex}=405$ nm) along with the fitted curve in (A) 130 mM DMB in D₂O and (B) 130 mM TMB in D₂O at 490 nm.

TABLE II. Anisotropy decay parameters of C153 in 130 mM DMB and TMB in D₂O and H₂O at $\lambda_{ex}=405$ nm.

System		r_0	Decay parameters of $r(t)$		$\langle \tau_{rot} \rangle^b$ (ps)	Hydrodynamic diameter (1:1) ^c (Å)	Hydrodynamic diameter (1:2) ^c (Å)
			τ_{fast}^a (ps) (a_{fast})	τ_{slow}^a (ps) (a_{slow})			
C153-DMB	D ₂ O	0.36	1450 (0.28)	3600 (0.72)	3000	17	22
	H ₂ O	0.35	1150 (0.33)	2700 (0.67)	2200	17	23
C153-TMB	D ₂ O	0.35	1000 (0.16)	3150 (0.84)	2800	15	22
	H ₂ O	0.34	1000 (0.20)	2500 (0.80)	2200	16	22

^a $\pm 10\%$.^b $\langle \tau_{rot} \rangle = a_{fast} \tau_{fast} + a_{slow} \tau_{slow}$.^c ± 1 Å.

The biexponential anisotropy decay of C153 bound to DMB and TMB may originate from the 1:1 and 1:2 complexes. The faster component may be ascribed to the smaller 1:1 complex and slower to the larger 1:2 complexes. From the time constant of anisotropy decay (τ_R) hydrodynamic radius (r_h) may be evaluated from the following relation:

$$\tau_R = \frac{4\pi\eta r_h^3}{3KT} \quad (7)$$

The slower rotation of C153 bound to DMB and TMB in D₂O compared to H₂O may be ascribed to nearly 25% times higher viscosity in D₂O compared to H₂O. Using the viscosity of 130 mM DMB in D₂O at 20 °C (~ 2.2 mPa s) and the faster component of anisotropy decay, the hydrodynamic radius (r_h) for 1:1 complex is estimated to be 8.5 Å for DMB (Table II). This corresponds to a length ($2r_h$) of 17 ± 1 Å. Since the height of the DMB cavity is 11 Å, the 17 Å length of the 1:1 complex suggests that a portion (6 Å) of the probe is projected out of the cavity. For 130 mM TMB in D₂O, the viscosity is found to be similar to that of 130 mM DMB and the hydrodynamic diameter is determined to be ~ 15 Å (Table II) which implies that ~ 4 Å of the probe (C153) is projected out of the cavity.

From the slower component of anisotropy decay (3600 ps for DMB and 3150 ps for TMB) the hydrodynamic radius (r_h) of the 1:2 complex for both DMB and TMB are determined to be ~ 11 Å corresponding to a diameter ($2r_h$) of ~ 22 Å. This is roughly equal to the sum of the height of two cavities joined together.

In summary, the slower anisotropy decay of C153-

cyclodextrin complex in D₂O is due to $\sim 25\%$ higher viscosity of D₂O. The sizes of the 1:1 and 1:2 (C153: CD) complexes in D₂O are similar to those²⁹ in H₂O.

C. Solvation dynamics of C153 bound to DMB and TMB in D₂O

The fluorescence decay of C153 exhibits strong isotope effect. Figure 6 shows the fluorescence decays of C153 in 130 mM DMB and TMB for H₂O and D₂O at $\lambda_{em}=620$ nm. The fluorescence decays of C153 bound to the cyclodextrin is longer in D₂O than those in H₂O. For C153 bound to DMB, the longest component of decay (~ 6 ns) in D₂O is longer than that in H₂O (~ 4.5 ns). The longer excited state decay (lifetime) of C153 bound to cyclodextrin in D₂O indicates retardation of the nonradiative process.⁵⁶ This is consistent with the increase in steady state emission quantum yield. This implies strong solvent (water)-solute coupling between C153 and H₂O (or D₂O) inside or near the cyclodextrin cavity.

The picosecond and femtosecond fluorescence transients of C153 in 130 mM DMB and TMB in D₂O are shown in Figs. 7 and 8. The emission transient of C153 exhibits a rise at the red end and decay at the blue end of the spectrum. This is a clear signature of solvation dynamics. For C153 bound to DMB in D₂O, the long rise time (650 ps) at the red end ($\lambda_{em}=600$ nm) of the fluorescence decay is longer than that (550 ps) in H₂O. Similarly, for C153 bound to TMB, the rise time in D₂O is longer than that in H₂O. The longer rise times indicate slower solvation of confined D₂O compared to confined H₂O.

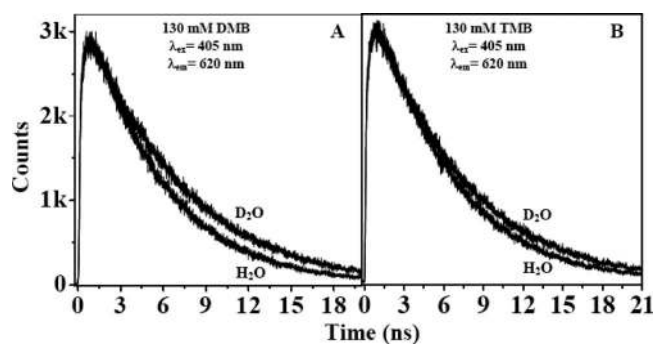


FIG. 6. Picosecond decay of C153 ($\lambda_{ex}=405$ nm) in (A) 130 mM DMB and (B) 130 mM TMB at $\lambda_{em}=620$ nm in both D₂O and H₂O.

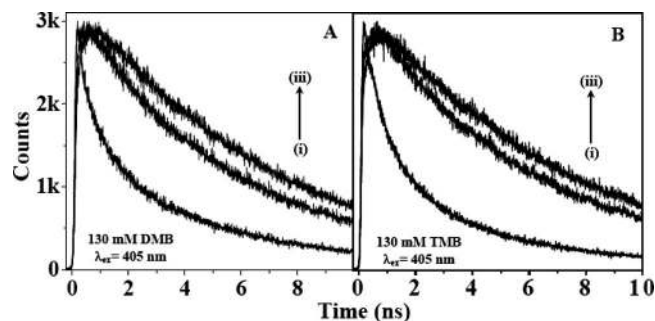


FIG. 7. Picosecond decay of C153 ($\lambda_{ex}=405$ nm) in (A) 130 mM DMB in D₂O and (B) 130 mM TMB in D₂O at $\lambda_{em}=(i)$ 460 nm, (ii) 520 nm, and (iii) 600 nm.

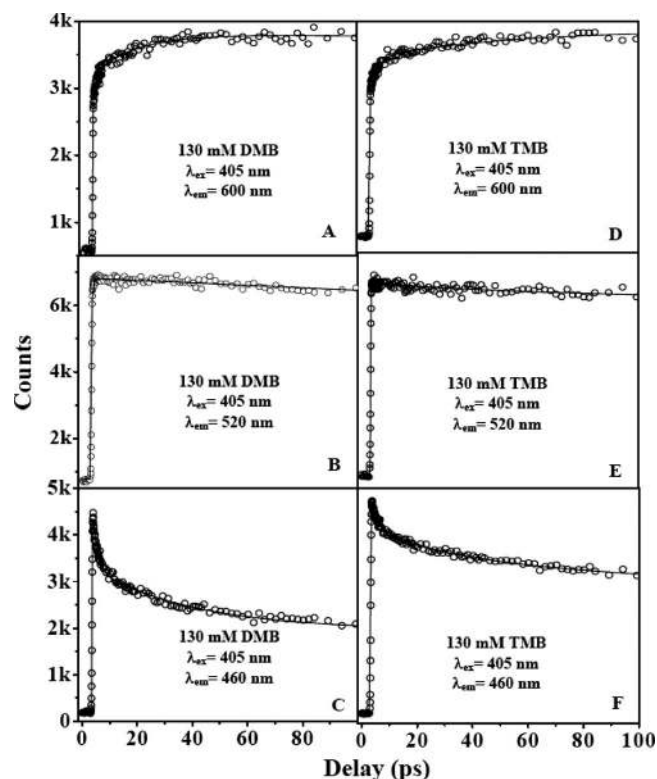


FIG. 8. Femtosecond fluorescence transient of C153 ($\lambda_{ex}=405$ nm) in the presence of 130 mM DMB in D₂O [(A)–(C)] and in the presence of 130 mM TMB in D₂O [(D)–(F)]; λ_{em} at 600 nm [(A) and (D)], 520 nm [(B) and (E)], and 460 nm [(C) and (F)].

Figure 9 shows the decay of $\nu(t)$ versus time (t) for C153 bound to DMB (and TMB) in both D₂O and H₂O. Figures 10 and 11 show the decay of solvent response function, $C(t)$ for C153 bound to DMB (and TMB). Table III summarizes the decay parameters of $C(t)$ for C153 in DMB (and TMB) and the dynamic solvent shift (DSS).

Using the Fee–Maroncelli method⁶⁷ and cyclohexane as the nonpolar solvent, it is calculated that for C153 bound to DMB in H₂O, 43% of the solvation dynamics was missed in our femtosecond setup. There are three components—2.4 ps (15%), 50 ps (17%), 1450 ps (25%) with average solvation time ($\langle\tau_S\rangle$) 375 ps. In D₂O, for C153 bound to DMB, 30% of the solvation dynamics was missed in our setup. In this case, decay of $C(t)$ exhibits three components—3.5 ps (19%), 150 ps (20%), 2000 ps (31%) with $\langle\tau_S\rangle=650$ ps (Table III). This shows that for C153 bound to DMB the solvation dynamics in D₂O is 1.7 times slower compared to that in H₂O. The total Stokes shift (DSS) for DMB in D₂O is found to be 525 cm⁻¹ which is larger than that (375 cm⁻¹) in H₂O.

For C153 bound to TMB in H₂O, 30% of the solvation dynamics was missed in our femtosecond setup. In this case, the decay of $C(t)$ exhibits three components—10 ps (25%), 240 ps (15%), 2450 ps (30%) with $\langle\tau_S\rangle=750$ ps. In D₂O, 20% of the solvation dynamics was missed and the decay components are 15 ps (34%), 300 ps (8%), 3000 ps (38%), and $\langle\tau_S\rangle=1150$ ps. This shows that for C153 bound to TMB the solvation dynamics in D₂O is 1.5 times slower compared to that in H₂O. The total Stokes shift for C153 bound to TMB in D₂O (750 cm⁻¹, Table III) is larger than that (650 cm⁻¹) in H₂O.

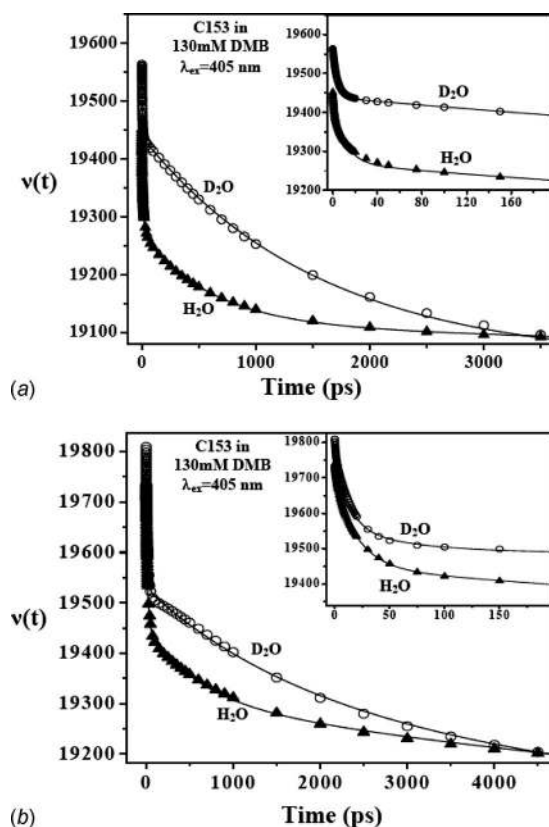


FIG. 9. Decay of $\nu(t)$ vs time (t) for C153 ($\lambda_{ex}=405$ nm) bound to (A) 130 mM DMB and (B) 130 mM TMB in H₂O (\blacktriangle) and in D₂O (\circ). The points denote the actual values of $\nu(t)$ and the solid line denotes the best fit to an exponential decay. Initial parts of the decays of $\nu(t)$ are shown in the inset.

We have studied the solvation dynamics of C480 in bulk H₂O and D₂O in our femtosecond upconversion set up. We obtained a very small (2% in H₂O and 4% in D₂O) fast component 150 fs (0.15 ps) in D₂O and 200 fs in water and 2 ps (17% in H₂O and 25% in D₂O).⁷⁰

IV. DISCUSSION

The marked deuterium isotope effect on C153 bound to cyclodextrin may be summarized as follows. First, the non-radiative decay of C153 bound to methylated cyclodextrin (DMB and TMB) is retarded (as shown by the increase in ϕ_f and τ_f). Second, the binding constants of C153 to both the cyclodextrins are found to be higher in D₂O compared to H₂O. Third, the solvation dynamics inside the cyclodextrin cavity is slowed down in D₂O compared to H₂O. Fourth, there is considerable difference in solvation dynamics between DMB and TMB (in both D₂O and H₂O). Fifth, the anisotropy decay of C153 bound to DMB (and TMB) in D₂O is slower than that in H₂O.

The slower nonradiative decay implies significant coupling between confined D₂O (and also H₂O) and the probe (C153) in the cyclodextrin cavity. The slower nonradiative decay arises from the energy gap law of nonradiative transition and the fact that slower solvation in D₂O keeps energy gap (between ground and excited state) large for a longer time.⁵⁶

The higher binding constant in D₂O arises from strong hydrophobic effect in D₂O. We have already indicated that

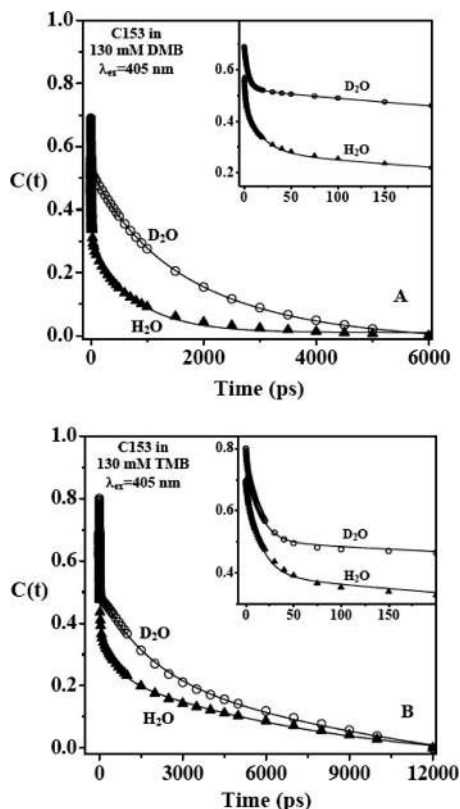


FIG. 10. Complete decay of solvent response function, $C(t)$ of C153 ($\lambda_{\text{ex}} = 405$ nm) bound to (A) 130 mM DMB and (B) 130 mM TMB in H_2O (\blacktriangle) and in D_2O (\circ). The points denote the actual values of $C(t)$ and the solid line denotes the best fit to an exponential decay. Initial parts of the decays of $C(t)$ are shown in the inset.

D_2O is more structured than H_2O . The hydrophobic effect arises mainly from the differences in water-water and water-organic hydrogen bonds. Since D_2O – D_2O hydrogen bonded structure is more stable (relative to H_2O), the hydrophobic aggregation (binding of C153 to DMB and TMB) is more favored in D_2O .

Shikata *et al.*⁷¹ studied dielectric relaxation of an aqueous solution of DMB and TMB. They detected three dielectric relaxation times (τ_D)—8, 20, and 2000 ps.⁷¹ The fastest

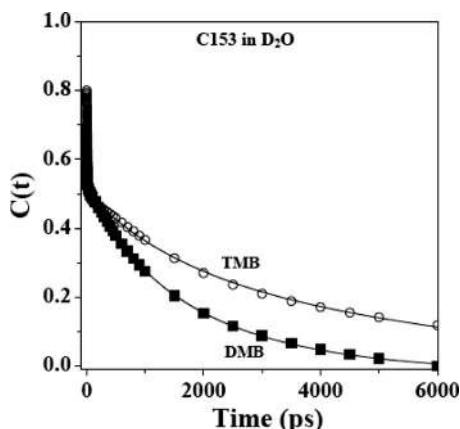


FIG. 11. Complete decay of solvent response function, $C(t)$ of C153 ($\lambda_{\text{ex}} = 405$ nm) bound to 130 mM DMB (\blacksquare) and 130 mM TMB (\circ) in D_2O . The points denote the actual values of $C(t)$ and the solid line denotes the best fit to an exponential decay.

component (8 ps) corresponds to bulk water.⁵⁴ The second (~ 20 ps) component is attributed to the exchange of bound and free water as envisaged by Nandi and Bagchi.⁷² The slowest nanosecond component (2000–2400 ps) is ascribed to overall tumbling (rotation) of the methylated cyclodextrin.⁷¹ These authors, however, did not study any deuterium isotope effect on dielectric relaxation of aqueous DMB and TMB. Note, dielectric relaxation of bulk D_2O is 25% slower than that of H_2O .⁵⁴

According to the dielectric continuum model, the solvation time (τ_s) corresponds to the longitudinal relaxation time, $(\epsilon_\infty/\epsilon_0)\tau_D$ and is smaller than the dielectric relaxation (τ_D) time by a factor $(\epsilon_\infty/\epsilon_0)$.⁷³ The emission maximum (522–525 nm) of C153 in methylated cyclodextrin is slightly blue-shifted to that (531 nm) (Ref. 68) in ethanol. Thus the static polarity (ϵ_0) is slightly less than that (25) in ethanol. If one assumes ϵ_∞ same as that (~ 4.5) (Ref. 73) in water, the solvation time in DMB and TMB is estimated to be about five times less than the dielectric relaxation time. Thus, the longest component of solvation in methyl cyclodextrin would be around $2000/4.5 \approx 500$ ps. This is much shorter than the 2000 ps component in DMB (3000 ps in TMB) observed in our work.

We propose the following model to explain the longest component (Table III) of solvation dynamics (2000 ps, 1450 ps for DMB and 3000 ps, 2450 ps for TMB). On excitation, the dipole moment of the probe (C153) increases and hence, it may move out of the hydrophobic cavity to the more polar environment outside. Such a self-motion (i.e., translation) of the probe from a less polar region to a more polar region has been predicted in computer simulation⁷⁴ and leads to spectral narrowing as is observed in the case of motion of a dye molecule (DCM) from interface to core of the water pool in a microemulsion.⁷⁵ Thus, we ascribe the longest component to self-diffusion of C153 out of the cyclodextrin cavity. The translational diffusion coefficient of C153 in an organized assembly may be obtained from analyzing the anisotropy data using wobbling-in-cone model.^{76–82} This model involves translation of a dye along the surface of the micelle. We have previously determined D_t of C153 in a neutral micelle ($\sim 1.75 \times 10^{-9}$ m² s⁻¹).⁷⁶ This corresponds to a distance ($\sqrt{2D_t t}$) 2 nm in 1450 ps and 3 nm in 3000 ps. Note, the 2–3 nm diffusion length is of the order of the length of a 1:2 (C153:CD) complex. Hence, the long component may arise from motion of the probe (C153) out of such a 1:2 complex (which contains major portion of the bound C153 molecules). Note, the ultraslow component increases from 1450 to 2000 ps for DMB and from 2450 to 3000 ps in TMB. This may be ascribed to the slower translational diffusion in D_2O and is correlated with the slower rotational diffusion in D_2O (as revealed in anisotropy decay).

The most important observation is the slowing down of solvation dynamics in the cyclodextrin cavity in D_2O compared to H_2O . For C153 bound to DMB, the average solvation time in D_2O is 1.7 times slower than that in water. For TMB, the slowing down is 1.5 times. The slowing down of the ultrafast component of solvation dynamics may be due to lowering of librational frequency as proposed^{55,56} in the case of bulk H_2O . The longest component of solvation arises

TABLE III. Decay parameters of $C(t)$ of C153 in 130 mM DMB and TMB in D_2O and H_2O at $\lambda_{ex}=405$ nm.

System		$\Delta\nu_{obs}^a$ [$\nu(0)$] (cm^{-1})	Decay parameter of $C(t)$	
			τ_i^b (a_i) (ps)	$\langle\tau_s\rangle$ (ps)
C153-DMB	D_2O	525 (19 560)	<0.3 (30%), ^c 3.5 (19%), 150 (20%), 2000 (31%)	650
	H_2O	375 (19 450)	<0.3 (43%), ^c 2.4 (15%), 50 (17%), 1450 (25%)	375
C153-TMB	D_2O	750 (19 810)	<0.3 (20%), ^c 15 (34%), 300 (8%), 3000 (38%)	1150
	H_2O	650 (19 740)	<0.3 (30%), ^c 10 (25%), 240 (15%), 2450 (30%)	750

^a $\Delta\nu_{obs}=[\nu(0)-\nu(\infty)]$, ± 100 cm^{-1} .^b $\pm 10\%$.^cCalculated using Fee–Maroncelli method (Ref. 67).

mainly from the increase in the excited state lifetime of the probe. The longest component of solvation dynamics inside the cyclodextrin cavity is on the order of excited state lifetime of the probe (C153). The longer excited state lifetime of C153 in D_2O causes an increase in the contribution of the ultraslow component of solvation. The increased contribution of the ultraslow component makes overall solvation slower in D_2O .

Solvation dynamics in TMB is found to be slower than that in DMB. This may be understood as follows. The emission maximum of C153 in DMB (525 nm) is blueshifted to that (522 nm) in TMB. This suggests that the probe resides in a more exposed (to bulk water or the clathratelike network) region in DMB and in TMB, it remains in a more buried location. The binding constant of C153 to TMB is, respectively, six times (for 1:1) and ten times (1:2) larger than those in DMB. This also suggests that the probe (C153) binds more strongly and presumably to a more hydrophobic location in TMB compared to DMB. Obviously solvation dynamics will be faster in a more exposed region, i.e., in DMB.

The slower anisotropy decay for C153 bound to the cyclodextrin is less surprising and may be due to higher viscosity of D_2O .

V. CONCLUSION

This work demonstrates that C153 bound to two cyclodextrin, exhibits marked deuterium isotope effect. This is manifested in slower nonradiative decay (longer excited state lifetime and higher ϕ_f) and slower solvation dynamics. The deuterium isotope effect suggests strong coupling between the probe C153 and water (H_2O and D_2O) inside the cyclodextrin cavity. The deuterium isotope effect confirms that confined water is mainly responsible for slow solvation dynamics in the DMB and TMB cavity. The slowest component of solvation may arise from translational diffusion of the probe out of the cyclodextrin cavity. The rotational and translational diffusion are slower in D_2O .

ACKNOWLEDGMENTS

Thanks are due to the Department of Science and Technology, India (Project No. IR/I1/CF-01/2002 and J. C. Bose Fellowship) for generous research support. D.K.S., S.D., and D.K.D. thank Council for Scientific and Industrial Research (CSIR) for awarding fellowships.

- ¹B. Bagchi, *Chem. Rev. (Washington, D.C.)* **105**, 3197 (2005).
- ²S. K. Pal and A. H. Zewail, *Chem. Rev. (Washington, D.C.)* **104**, 2099 (2004).
- ³K. Bhattacharyya, *Chem. Commun. (Cambridge)* 2848 (2008).
- ⁴B. Baruah, J. M. Roden, M. Sedgwick, N. M. Correa, C. D. Crans, and N. E. Levinger, *J. Am. Chem. Soc.* **128**, 12758 (2006).
- ⁵R. E. Riter, D. M. Willard, and N. E. Levinger, *J. Phys. Chem. B* **102**, 2705 (1998).
- ⁶R. E. Riter, E. P. Undiks, and N. E. Levinger, *J. Am. Chem. Soc.* **120**, 6062 (1998).
- ⁷N. M. Correa and N. E. Levinger, *J. Phys. Chem. B* **110**, 13050 (2006).
- ⁸D. Pant and N. E. Levinger, *Langmuir* **16**, 10123 (2000).
- ⁹N. E. Levinger, *Curr. Opin. Colloid Interface Sci.* **5**, 118 (2000).
- ¹⁰L. Frauchiger, H. Shirota, K. E. Uhrich, and E. W. Castner, Jr., *J. Phys. Chem. B* **103**, 7846 (2002).
- ¹¹H. Shirota and E. W. Castner, Jr., *J. Am. Chem. Soc.* **123**, 12877 (2001).
- ¹²H. Shirota and K. Horie, *J. Phys. Chem. B* **103**, 1437 (1999).
- ¹³W. Qiu, L. Zhang, O. Okobiah, Y. Yang, L. Wang, D. Zhong, and A. H. Zewail, *J. Phys. Chem. B* **110**, 10540 (2006).
- ¹⁴J. Kim, W. Lu, W. Qiu, L. Wang, M. Caffrey, and D. Zhong, *J. Phys. Chem. B* **110**, 21994 (2006).
- ¹⁵P. Mukherjee, J. A. Crank, M. Halder, D. W. Armstrong, and J. W. Petrich, *J. Phys. Chem. A* **110**, 10725 (2006).
- ¹⁶M. Halder, K. Das, P. K. Chowdhury, S. Kundu, M. S. Hargrove, and J. W. Petrich, *J. Phys. Chem. B* **107**, 9933 (2003).
- ¹⁷P. Hazra, D. Chakrabarty, and N. Sarkar, *Chem. Phys. Lett.* **371**, 553 (2003).
- ¹⁸P. Hazra, D. Chakrabarty, and N. Sarkar, *Langmuir* **18**, 7872 (2002).
- ¹⁹P. Hazra and N. Sarkar, *Chem. Phys. Lett.* **342**, 303 (2001).
- ²⁰D. Banerjee and S. K. Pal, *Chem. Phys. Lett.* **451**, 237 (2008).
- ²¹R. K. Mitra, S. S. Sinha, and S. K. Pal, *Langmuir* **24**, 49 (2002).
- ²²R. K. Mitra, S. S. Sinha, and S. K. Pal, *J. Phys. Chem. B* **111**, 7577 (2007).
- ²³M. Kumbhakar, T. Goel, T. Mukherjee, and H. Pal, *J. Phys. Chem. B* **109**, 18528 (2005).
- ²⁴S. Bandyopadhyay, S. Chakraborty, S. Balasubramanian, and B. Bagchi, *J. Am. Chem. Soc.* **127**, 4071 (2005).
- ²⁵S. Bandyopadhyay, S. Chakraborty, and B. Bagchi, *J. Am. Chem. Soc.* **127**, 16660 (2005).
- ²⁶S. K. Sinha, S. Chakraborty, and S. Bandyopadhyay, *J. Phys. Chem. B* **112**, 8203 (2008).
- ²⁷D. Andreatta, S. Sen, J. L. P. Lustres, S. A. Kovalenko, N. P. Ernsting, C. J. Murphy, R. S. Coleman, and M. A. Berg, *J. Am. Chem. Soc.* **128**, 6885 (2006).
- ²⁸S. Vajda, R. Jimenez, S. J. Rosenthal, V. Fidler, G. R. Fleming, and E. W. Castner, Jr., *J. Chem. Soc., Faraday Trans.* **91**, 867 (1995).
- ²⁹P. Sen, D. Roy, S. K. Mondal, K. Sahu, S. Ghosh, and K. Bhattacharyya, *J. Phys. Chem. A* **109**, 9716 (2005).
- ³⁰N. Nandi and B. Bagchi, *J. Phys. Chem. B* **101**, 10954 (1997).
- ³¹N. Nandi and B. Bagchi, *J. Phys. Chem.* **100**, 13914 (1996).
- ³²S. Senapati and A. Chandra, *J. Phys. Chem. B* **105**, 5106 (2001).
- ³³T. S. Gulmen and W. H. Thompson, *Langmuir* **22**, 10919 (2006).
- ³⁴J. A. Gomez and W. H. Thompson, *J. Phys. Chem. B* **108**, 20144 (2004).
- ³⁵J. Faeder and B. M. Ladanyi, *J. Phys. Chem. B* **109**, 6732 (2005).
- ³⁶M. R. Harpham, B. M. Ladanyi, and N. E. Levinger, *J. Phys. Chem. B* **109**, 16891 (2005).
- ³⁷S. Pal, B. Bagchi, and S. Balasubramanian, *J. Phys. Chem. B* **109**, 12879

- (2005).
- ³⁸ S. Senapati and M. L. Berkowitz, *J. Chem. Phys.* **118**, 1937 (2003).
- ³⁹ F. Pizzitutti, M. Marchi, F. Sterpone, and P. J. Rossky, *J. Phys. Chem. B* **111**, 7584 (2007).
- ⁴⁰ T. Li, A. A. Hassanali, Y.-T. Kao, D. Zhong, and S. J. Singer, *J. Am. Chem. Soc.* **129**, 3376 (2007).
- ⁴¹ A. A. Golosov and M. Karplus, *J. Phys. Chem. B* **111**, 1482 (2007).
- ⁴² J. Rodriguez, J. Marti, E. Guardia, and D. Laria, *J. Phys. Chem. B* **112**, 8990 (2008).
- ⁴³ A. K. Soper and C. J. Benmore, *Phys. Rev. Lett.* **101**, 065502 (2008).
- ⁴⁴ G. Nemethy and H. A. Scheraga, *J. Chem. Phys.* **41**, 680 (1964).
- ⁴⁵ M. V. Rekharsky and Y. Inoue, *J. Am. Chem. Soc.* **124**, 12361 (2002).
- ⁴⁶ A. S. Wang and Y. Matsui, *Bull. Chem. Soc. Jpn.* **67**, 2917 (1994).
- ⁴⁷ D. Pant and N. E. Levinger, *Phys. Chem. B* **103**, 7846 (1999).
- ⁴⁸ E. W. Castner, Jr., Y. J. Chang, Y. C. Chu, and G. E. Walfaren, *J. Chem. Phys.* **102**, 653 (1995).
- ⁴⁹ P. J. Reid and P. F. Barabar, *J. Phys. Chem.* **99**, 3554 (1995).
- ⁵⁰ H. Shirota, H. Pal, K. Tominaga, and K. Yosihara, *J. Phys. Chem.* **100**, 14575 (1996).
- ⁵¹ H. Shirota, Y. Tamato, and H. Segawa, *J. Phys. Chem. A* **108**, 3244 (2004).
- ⁵² S. Das, A. Datta, and K. Bhattacharyya, *J. Phys. Chem. A* **101**, 3299 (1997).
- ⁵³ B. Zolotov, A. Gan, B. D. Feinberg, and D. Huppert, *Chem. Phys. Lett.* **265**, 418 (1997).
- ⁵⁴ U. Kaatz, *Chem. Phys. Lett.* **203**, 1 (1993).
- ⁵⁵ N. Nandi, S. Roy, and B. Bagchi, *J. Chem. Phys.* **102**, 1390 (1995).
- ⁵⁶ B. J. Schwartz and P. J. Rossky, *J. Chem. Phys.* **105**, 6997 (1996).
- ⁵⁷ R. Jimenez, G. R. Fleming, P. V. Kumar, and M. Maroncelli, *Nature (London)* **369**, 471 (1994).
- ⁵⁸ C. J. Fecko, J. D. Eaves, J. J. Loparo, A. Tokmakoff, and P. L. Geissler, *Science* **301**, 1698 (2003).
- ⁵⁹ W. Jarzeba, G. C. Walker, A. E. Johnson, M. A. Kahlow, and P. F. Barabar, *J. Phys. Chem.* **92**, 7039 (1988).
- ⁶⁰ F. O. Ortega-Caballero, C. O. Mellet, L. L. Gourrierc, N. Guilloteau, C. D. Giorgio, P. Vierling, J. Defaye, and J. M. G. Fernandez, *Org. Lett.* **10**, 5143 (2008).
- ⁶¹ M. Khajepour, T. Troxler, V. Nanda, and J. M. Vanderkooi, *Proteins* **55**, 275 (2004).
- ⁶² E. B. Starikov, K. Brasicke, E. W. Knapp, and W. Saenger, *Chem. Phys. Lett.* **336**, 504 (2001).
- ⁶³ J. Frank, J. F. Holzwarth, and W. Saenger, *Langmuir* **18**, 5974 (2002).
- ⁶⁴ T. Aree, H. Hoier, B. Schulz, G. Reck, and W. Saenger, *Angew. Chem., Int. Ed.* **39**, 897 (2000).
- ⁶⁵ T. Steiner and W. Saenger, *Angew. Chem., Int. Ed.* **37**, 3404 (1998).
- ⁶⁶ M. Maroncelli and G. R. Fleming, *J. Chem. Phys.* **86**, 6221 (1987).
- ⁶⁷ R. S. Fee and M. Maroncelli, *Chem. Phys.* **183**, 235 (1994).
- ⁶⁸ G. Jones II, W. R. Jackson, C.-Y. Choi, and W. R. Bergmark, *J. Phys. Chem.* **89**, 294 (1985).
- ⁶⁹ P. Hazra, D. Chakrabarty, A. Chakraborty, and N. Sarkar, *Biochem. Biophys. Res. Commun.* **314**, 543 (2004).
- ⁷⁰ D. K. Das, D. K. Sasmal, A. Adhikari, and K. Bhattacharyya (unpublished).
- ⁷¹ T. Shikata, R. Takahashi, and Y. Satokawa, *J. Phys. Chem. B* **111**, 12239 (2007).
- ⁷² N. Nandi and B. Bagchi, *J. Phys. Chem. A* **102**, 8217 (1998).
- ⁷³ M. Maroncelli, *J. Mol. Liq.* **57**, 1 (1993).
- ⁷⁴ W. H. Thompson, *J. Chem. Phys.* **120**, 8125 (2004).
- ⁷⁵ P. Dutta, P. Sen, S. Mukherjee, A. Haldar, and K. Bhattacharyya, *J. Phys. Chem. B* **107**, 10815 (2003).
- ⁷⁶ S. Ghosh, S. K. Mondal, K. Sahu, and K. Bhattacharyya, *J. Chem. Phys.* **126**, 204708 (2007).
- ⁷⁷ P. Sen, S. Ghosh, K. Sahu, S. K. Mondal, D. Roy, and K. Bhattacharyya, *J. Chem. Phys.* **124**, 204905 (2006).
- ⁷⁸ E. L. Quitevis, A. H. Marcus, and M. D. Fayer, *J. Phys. Chem.* **97**, 5762 (1993).
- ⁷⁹ M. G. M. Krishna, R. Das, N. Periasamy, and R. Nityananda, *J. Chem. Phys.* **112**, 8502 (2000).
- ⁸⁰ N. W. Wittouck, R. M. Negri, and F. C. De Schryver, *J. Am. Chem. Soc.* **116**, 10601 (1994).
- ⁸¹ S. Sen, D. Sukul, P. Dutta, and K. Bhattacharyya, *J. Phys. Chem. A* **105**, 7495 (2001).
- ⁸² K. Bhattacharyya, *Acc. Chem. Res.* **36**, 95 (2003).